Calibration of External Electro-Optic Sampling Using Field Simulation and System Transfer Function Analysis

Xiaohua Wu, David Conn, Jian Song and Kent Nickerson

Communications Research Laboratory
McMaster University
Hamilton, Ontario, Canada L8S 4K1

Abstract

A field based calibration technique for external electro-optic (E-O) sampling has been proposed using the system transfer function approach and verified by simulation. The optical simulation incorporated with the Finite-Difference Time-Domain (FD-TD) full wave field analysis is used to predict the optical output in external E-O sampling and to evaluate the system transfer function. This calibration technique will enable us to de-embed the distortion in E-O sampling and to move E-O sampling further towards quantitative measurements. It is found that distortions can be introduced by probes due to their intrinsic frequency response determined by probe dimensions and materials. Generally, it is confirmed that thin probes exhibit less distortion in picosecond or subpicosecond measurements.

1 Introduction

External Electro-optic (E-O) sampling has shown promising results in characterizing monolithic microwave integrated circuits (MMICs) as well as other very high speed electronics devices. This is because of its high frequency capability and noninvasive property in measurements of internal signals in MMICs. However, little attention has been given to the accuracy or quantitative measurement of this technique. This paper has developed a general field based calibration technique for external E-O sampling systems using a system transfer function obtained from the field simulation results in the FD-TD method incorporated with optical electronics. It enables us to de-embed the distortion in external E-O sampling and to move E-O sampling further towards the quantitative measurement.

Previously, we have discussed the invasiveness and the distortion in external E-O sampling measurement in field and wave point of view [1][2]. It is desirable to develop a calibration technique to *de-embed* the distortion from the sampling measurement results and to *evaluate* the invasiveness to the device under test. The new calibration technique is based on the calculation of the E-O effects in the probes by optical electronics incorporated with the field simulations. First, the fields and waves have been simulated in a E-O sampling system when a very short Gaussian pulse is launched down to a coplanar waveguide (CPW). Then, the response has been used to calculate the E-O sampling output using electro-optic tensor of probes and other techniques in optical electronics. On this basis, a system transfer function is found in terms of the *input*, the electric field in the device under test, and the optical *output* (the change in polarization of the sampling beam). Finally, using this system transfer function and deconvolution technique, an electric field response in the device under test can be quantitatively related to a corresponding optical output in external E-O sampling.

2 Light intensity calculation

The FD-TD full wave field simulation in E-O sampling, as shown in Fig. 1, is based on the Terametrics Model 200 probe, where $LiTaO_3$ is used for probe material [1]. The simulation deals with a 0.6 ps full-width at half-maximum (FWHM) Gaussian pulse launched in the z-direction towards the probe with an applied voltage of $1V$. The parameters of the simulation can be found in [1].

E-O measurements are ultimately made through the change in the probe tip's birefringence with respect to the sampling laser beam. Unfortunately, significant electric field distortion in the optical probe has been observed in our analysis [1]. In order to realize the highest response of the $LiTaO_3$ probe tip to the expected orientation of the CPW electric field, the optical axis of the tip was chosen parallel to the y-axis (Fig. 1).

The propagation of light through a birefringent crystal is fully described by the index ellipsoid [3], which is written as (1)

$$\begin{bmatrix} x \\ y \\ z \end{bmatrix}^T \begin{bmatrix} \left(\frac{1}{n^2}\right)_1 & \left(\frac{1}{n^2}\right)_6 & \left(\frac{1}{n^2}\right)_5 \\ \left(\frac{1}{n^2}\right)_6 & \left(\frac{1}{n^2}\right)_2 & \left(\frac{1}{n^2}\right)_4 \\ \left(\frac{1}{n^2}\right)_5 & \left(\frac{1}{n^2}\right)_4 & \left(\frac{1}{n^2}\right)_3 \end{bmatrix} \begin{bmatrix} x \\ y \\ z \end{bmatrix} = 1 \qquad (1)$$

The presence of an electric field on light propagation is described by changes of the constants $(\frac{1}{n^2})_i, i = 1, 2, ..., 6$, so that (1) becomes

$$\left(\frac{1}{n^2}\right)_i = \left(\frac{1}{n^2}\right)_i\Big|_{E=0} + \Delta\left(\frac{1}{n^2}\right)_i$$

OF1

CH3277-1/93/0000-0221$01.00 © 1993 IEEE

$$= \left(\frac{1}{n^2}\right)_i\Big|_{E=0} + \sum_{j=1}^{3} r_{ij}E_j \qquad (2)$$

where $i = 1, 2, ..., 6$ as shown in (1), $j = 1, 2, 3$ to correspond with x, y, z, and r_{ij} is an element of the electro-optic tensor for $LiTaO_3$, which can be found in [3].

In most studies presented in the literature, only one of the electric field components in (2 is considered significant [4][5]. From our three dimensional simulation, however, all electric field components are found to be comparable due to discontinuities induced by probing, so that all components must be considered.

The principal axes and corresponding refraction indices of a new index ellipsoid (3) is constructed from the eigenvalues of the coefficient matrix in (1). This yields

$$\left(\frac{x'}{n_{x'}}\right)^2 + \left(\frac{y'}{n_{y'}}\right)^2 + \left(\frac{z'}{n_{z'}}\right)^2 = 1 \qquad (3)$$

where $n_{x'}$,$n_{y'}$ and $n_{z'}$ are refraction indices along new principal axes.

In the FD-TD field simulation, Δt is the time step and $\Delta\ell_k$ the kth x-axis mesh size in the probe tip. If E-O probing is in the x-direction, the retardation $\Gamma_k(m)$ at instant $m\Delta t$ in the kth mesh within the probe tip due to the applied electric field is

$$\begin{aligned}\Gamma_k(m) &= 2(\varphi_z - \varphi_y) \\ &= \frac{4\pi}{\lambda}\left[n_{z'}(m) - n_{y'}(m)\right]\Delta\ell_k \qquad (4)\end{aligned}$$

where λ is the free space wavelength of the probing laser beam. The optical output $i_k(m)$ corresponding to $\Gamma_k(m)$ can be readily calculated from (4) [3].

In order to investigate the impact of the probe thickness on the external E-O sampling, the time for probing beam to pass through the probe has to be considered. The overall optical output at the instant $m\Delta t$ in external E-O sampling should be the integration of $i_k(m)$ at corresponding instant when the probing beam and the electric field are intercepted within the kth mesh. For convenience, 100% transparency and reflection are assumed respectively at the top $LiTaO_3$-Silica support interface and the output facet of the probe. The E-O effects contributing to the overall optical output at the instant $m\Delta t$ along incident and reflect paths can be respectively expressed as

$$i_{inc}(m) = \sum_{k=n_{tip}}^{1} i_k(m - \delta t)|_{\delta t=(n_{tip}+k)\tau} \qquad (5)$$

$$i_{ref}(m) = \sum_{k=1}^{n_{tip}} i_k(m - \delta t)|_{\delta t=k\tau} \qquad (6)$$

where n_{tip} is the number of the meshes in the probe tip and τ is time period taken by probing beam to pass through one mesh. $i_k(m\text{-}\delta t)$, however, may not available in the field simulation at any instant. In this case, the interpolation method is used to find its value. The overall optical output at the instant $m\Delta t$ in external E-O sampling can be found as

$$i_{all}(m) = i_{inc}(m) + i_{ref}(m) \qquad (7)$$

The integration of $i_{all}(m)$ at all time steps will provide the E-O response to the electric input in the device under test.

Fig. 2 shows the normalized optical output calculated in (7) for probe thickness of 20μm in the external E-O sampling as the response to an electric input, a 0.6 ps Gaussian pulse. The optical output can also be obtained by assuming that the interaction between the optical probing beam and the electric field in the probe takes place instantaneously. The optical output found with this assumption is also shown in Fig. 2 for comparison. It is apparent that for this geometry, the assumption is basically valid.

3 Transfer function and Calibration

A general field based calibration technique for external E-O sampling is proposed and verified using a system transfer function. It allows us to extend external E-O sampling performance to the subpicosecond domain where the significant distortion occurs due to the probing effects [1]. The zero-state response of a linear system to input f(t) is given by its system transfer function. E-O sampling systems can be described as a linear system since only linear E-O effects are involved. The system input is the electric field in the device under test while the output is the optical response in E-O sampling. The system distortion will be characterized by the transfer function and de-embedded for measurement of system input when the system transfer function and the output are given.

To characterize the E-O sampling system transfer function, the full wave field analysis and the optical output calculation are made for a given electric input. Then the system transfer function $H(\omega)$ can be easily evaluated in the frequency domain by (8).

$$I_{all}(\omega) = E_{DUT}(\omega)H(\omega) \qquad (8)$$

where $I_{all}(\omega)$ and $E_{DUT}(\omega)$ are the Fourier transform of the optical output $i_{all}(m)$ and the system electric input $e_{DUT}(m)$, respectively. e_{DUT} is known in calibration and $i_{all}(\omega)$ can be measured or calculated based on the field simulation results.

Given the system transfer function $H(\omega)$, the unknown electric input $e_{DUT}(t)$ corresponding to the measured optical output $i_{all}(\omega)$ can be determined by

$$e_{DUT}(t) = \mathcal{F}^{-1}\left[\frac{I_{all}(\omega)}{H_{sys}(\omega)}\right] \qquad (9)$$

where the probing distortion, the CPW's dispersion and the other parasitic effects with the system have been calibrated out.

4 Results

Fig. 3 shows the system transfer function of the external E-O sampling for the $LiTaO_3$ probe thickness of 20μm. An

approximate constant frequency response is observed below 200GHz, which ensures the distortionless measurement up to 2.5 ps range. The two resonant like peaks occur at 600GHz and 800GHz which may correspond to probe thickness and width, which may attribute to the distortion in external E-O sampling. It confirms that thinner probes result in less distortion in measurements [6]. A sharp decreasing in frequency response beyond 800GHz may suggest that a larger distortion in magnitude will be introduced using this probe for the measurement where the pulse cycle involved is in the order of subpicosecond.

To demonstrate applications of this system transfer function, a square wave signal is applied to the CPW. The corresponding optical output can be predicted using the system transfer function. Both the input square wave signal and the corresponding optical output are shown in Fig. 4. The E-O sampling output shows ringing tails at rising and falling edges of the response to the first square while exhibits a distortionless response to the second square. This is attributed to the fact that the frequency bandwidth of the second square in the electric input is limited to about 100GHz, which is well within the flat characteristic region of the probe (See Fig. 3).

Regarding calibration, the electric field in the device under test, as a response of interests and an input of E-O sampling systems, is to be determined by the measured optical output. A simulation has been made for verifying the proposed calibration technique, where a known 1.0 ps Gaussian pulse is launched down to the CPW. The optical output in the external E-O sampling is found in the FD-TD field simulation incorporated with E-O effect calculation. Using the obtained system transfer function, the electric input can be determined by (9). Fig. 5 gives an electric input (1.0 ps Gaussian pulse), its optical output in the external E-O sampling found in the optical and field simulations, and the input calculated by the proposed calibration method. Obviously, the excellent agreement confirms the validity of the calibration method.

5 Conclusions

A field based calibration technique for external E-O sampling has been developed and verified using the system transfer function. The E-O effects analysis and the FD-TD method have been used for the prediction of the optical output and the simulation of the full wave field in the external E-O sampling system. The traveling time taken for the probing beam to go through the probe was considered in the optical output calculations. It was found that for the probe thickness of 20 μm, this time period does not show noticeable effect on sampling results. A significant distortion may be introduced by probes for frequencies higher than 400GHz, which may vary for different dimensions of probes. Generally, it is confirmed that the thinner probe does show a flat characteristic in a wider frequency range, hence less distortion at higher frequencies or higher speed measurements.

References

[1] D. Conn, X. Wu, J. Song and K. Nickerson, "A full wave simulation of disturbances in picosecond signal by electro-optic sampling, " *1992 IEEE MTT-S Int. Microwave Symp. Dig.* (Albuquerque, NM), pp.665-668.

[2] X. Wu, J. Song, K. Nickerson and D. Conn, "Invasiveness of $LiTaO_3$ and GaAs probes in external electro-optic sampling," to be published in *IEEE/OSA J. Lightwave Tech.*.

[3] Amnon Yariv, *Optical Electronics*, Fourth edition, Philadelphia, Saunders College Publishing, 1991.

[4] T.Nagatsuma, T.Shibata, E.Sano, and A.Iwata, "Subpicosecond sampling using a noncontact electro-optic probe," *J.Appl. Phys.*, vol.66, pp.4001-4009, 1989.

[5] J.M. Wiesenfeld, "Electro-optic sampling of high-speed devices and integrated circuits," *IBM J. Res. Develop.*, vol.34, pp.141-161, 1990.

[6] M. Y. Frankel, J. F. Whitaker, G. A. Mourou and J. A. Valdmanis, "Experimental characterization of external electrooptic probes, " *IEEE Microwave & Guided Wave Lett.*, pp.60-62, Mar., 1991.

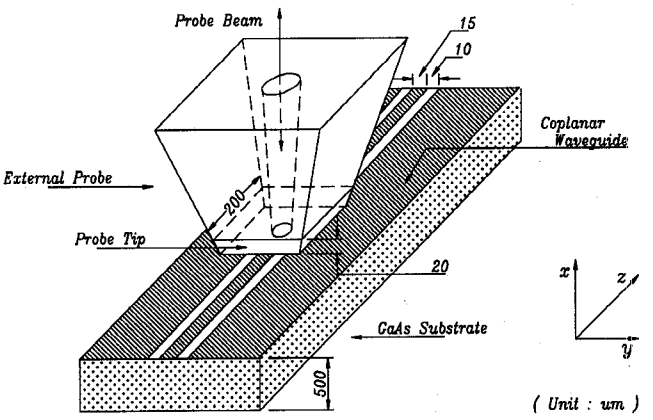

Figure 1: Schematic of the external electro-optic sampling configuration. The coplanar waveguide is the device under test. Probe tip material is $LiTaO_3$ and its optical axis is placed parallel to y-direction.

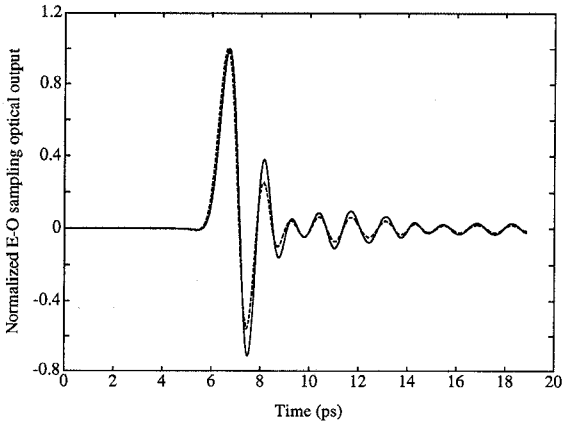

Figure 2: Normalized E-O sampling output response to a 0.6 ps Gaussian pulse propagating on the CPW. Solid line: when the traveling time taken for the probing beam to go through the probe is considered; Dashed line: when the simultaneous interaction between the optical beam and the electric field in the probe is assumed.

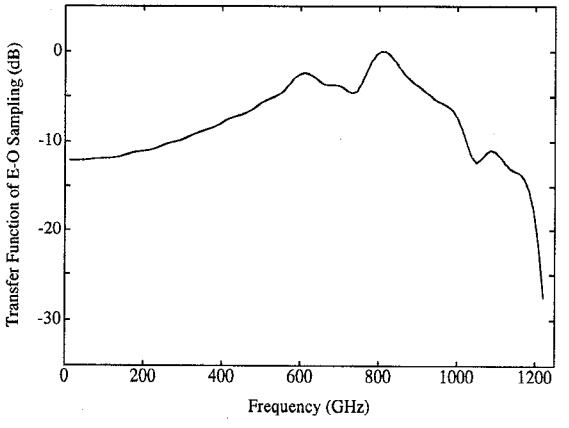

Figure 3: The system transfer function of the external E-O sampling for the $LiTaO_3$ probe thickness of $20\mu m$. An approximate constant frequency response up to 200GHz, two resonant like peaks at 600GHz and 800GHz, and a sharp decreasing in magnitude beyond 800GHz can be observed.

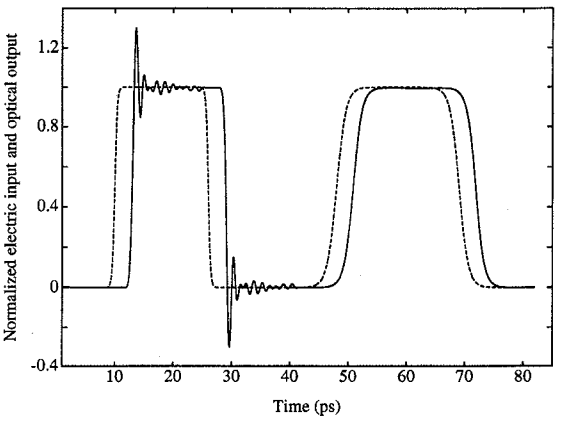

Figure 4: Comparison of a square wave signal propagating on the CPW and its E-O sampling output response. Solid line: E-O sampling output; Dashed line: electric input signal to the CPW. The E-O sampling output shows ringing tails at rising and falling edges of the first square while exhibits distortionless response to the second square. This is due to the fact that the first square of the input has relatively large frequency components beyond 200GHz, where the frequency response of the probe changes quickly (Fig. 3). A time delay in the optical output relative to the electric input is also observed.

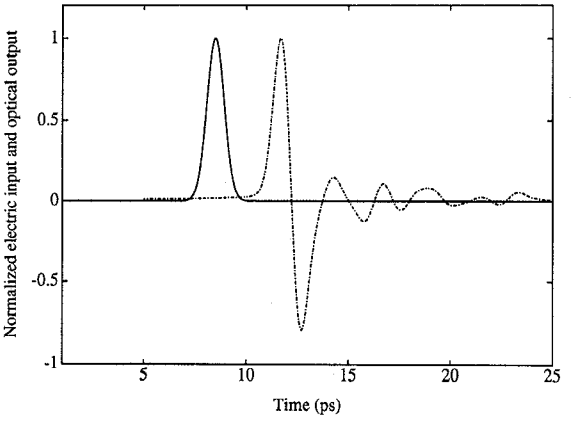

Figure 5: Comparison of the electric input obtained by the proposed calibration technique and the actual electric input. The optical output obtained by field and E-O effect simulation is also shown in this figure. Solid line: calculated electric input; Dashed line: the actual electric input; Dash-dot line: the corresponding uncorrected E-O system output. Solid line and dahsed line almost coincide with each other. It shows the excellent agreement between the calculated and the actual input signals. The ringing in the optical output is the sampling distortion to high frequency components.